# Combining CT Coronary Angiography and Myocardial Flow Reserve: Is It the Future?

11

Paul Knaapen

## 11.1 Introduction

Coronary artery disease (CAD) is the leading cause of death in the Western world. An accurate and early diagnosis is therefore warranted to determine the presence and extent of disease to guide clinical management. Invasive coronary angiography (ICA), in conjunction with intracoronary pressure measurements for intermediate coronary lesions, is considered the reference standard for this purpose [1]. With supreme temporal and spatial resolution, ICA provides reliable and accurate information on coronary luminal abnormalities. Furthermore, simultaneous assessment of fractional flow reserve (FFR) identifies patients who are eligible for revascularization, and FFR-driven percutaneous coronary intervention (PCI) improves outcome [2–4]. The invasive nature and high costs, however, warrant noninvasive screening to act as gatekeeper for conventional angiography and select those patients in whom obstructive CAD is most likely [5].

Coronary computed tomography angiography (CCTA) has recently emerged as a noninvasive alternative for its invasive counterpart to evaluate coronary anatomy [6]. The widespread availability of CT technology and ease of implementation in daily clinical practice has resulted in an exponential utilization of this imaging modality [7]. CCTA has proven particularly useful to exclude CAD due to its excellent sensitivity. Much like ICA, however, CCTA is a purely anatomical imaging technique, and hemodynamic consequences for a given epicardial cannot be determined, emphasizing the role of myocardial perfusion imaging (MPI) in the noninvasive evaluation of CAD [8]. Although several imaging modalities are available to assess myocardial perfusion, positron emission tomography (PET) has shown to possess the highest diagnostic accuracy to diagnose CAD [9–11]. Moreover,

P. Knaapen, MD
Department of Cardiology, VU University Medical Center of Amsterdam, Amsterdam, The Netherlands
e-mail: p.knaapen@vumc.nl



T.H. Schindler et al. (eds.), *Molecular and Multimodality Imaging in Cardiovascular Disease*, DOI 10.1007/978-3-319-19611-4_11

PEt allows to quantify myocardial blood flow (MBF) and flow reserve (MFR) in absolute terms, which adds important diagnostic and prognostic value in the evaluation of patients with (suspected) CAD. Due to its limited availability, methodological complexity, and high cost, cardiac PET has long been considered to be a research tool only. With the introduction of hybrid PET/CT, predominantly driven by its success in clinical oncology, cardiac PET is becoming increasingly available. This growth in hardware has been paralleled by improvements in radiotracer availability and advances in post-processing software. Consequently, cardiac PET has witnessed more widespread use and routine implementation in the clinical arena. Moreover, these hybrid devices now allow to acquire anatomical and functional information of the coronary tree in a single imaging session [12]. This chapter will discuss the advantages of hybrid imaging with PET/CT and quantification of flow over each modality separately in patients suspected of CAD.

## 11.2 Coronary Computed Tomography Angiography

Over the last decade, CCTA has developed as a valuable noninvasive alternative for the visualization of coronary anatomy. Current multislice CT scanners in combination with modern acquisition protocols enable robust and reproducible assessment of coronary artery morphology with relatively high temporal and spatial resolution accomplished at acceptable radiation dose [13]. The diagnostic accuracy of CCTA has been extensively studied, and pooled analysis of the literature demonstrates a consistent and unequaled high sensitivity (96 %) and negative predictive value (NPV, 94 %), positioning CCTA as a perfect tool to rule out CAD [14]. This holds particularly true in patients with a low pretest likelihood of disease. In contrast, specificity (76 %) and positive predictive value (PPV, 84 %) are generally moderate [14]. Lesion assessment is less accurate in comparison with ICA owing to the lower spatial and temporal resolution. Image quality is further affected by several additional factors such as heart rate and rhythm, body size, motion artifacts, quality of contrast opacification, and coronary calcifications. Although proper patient selection, preparation, and tailored imaging protocols can optimize image quality, coronary calcification is unamendable. The latter causes blooming artifacts and systemic overestimation of lesion severity [15]. Dual-energy CT acquisitions may reduce this issue, yet both invasive and noninvasive coronary imaging of a stenosis will continuously fail to accurately predict its functional aspects [16]. Hybrid imaging studies have shown that of CCTA deemed positive scans, approximately only half are actually associated with perfusion defects as documented with nuclear MPI [8, 17, 18]. Therefore, functional assessment is mandatory in the presence of an apparent obstructive stenosis to discern its hemodynamic relevance. Of interest, studies have unequivocally demonstrated that CCTA as an initial diagnostic test conveys increased downstream test utilization, costs, as well as revascularization procedures without a clear benefit in outcome [19–21].

The prognostic value of CCTA beyond traditional risk factors has been well documented, whereby adverse cardiac events are extremely rare in case of normal

findings, and risk gradually increases in line with the extent of CAD [22–24]. An additional advantage of CT-based angiography is the fact that plaque morphology can be assessed. Noncalcified plaques are shown to bear an unfavorable prognosis. Noncalcified lesions, although not necessarily of obstructive nature impeding myocardial perfusion, are associated with plaque vulnerability and the occurrence of acute coronary syndromes due to plaque rupture [25–27]. The clinical implications of these observations are under investigation, and the impact of preventive medical strategies instigated by the detection of CT-graded nonobstructive CAD on outcome remains to be elucidated.

## 11.3 Positron Emission Tomography

Positron emission tomography (PET) is widely accepted as the reference technique to assess myocardial perfusion noninvasively in vivo [28]. For this purpose, four tracers in particular have been validated. Of the available tracers, $^{82}$Rb, $^{13}NH_3$, and $H_2{}^{15}O$ are the most commonly used for the assessment of myocardial perfusion [29]. $^{18}$F-flurpiridaz is an emerging perfusion tracer not yet available for clinical use, but holds great potential and is currently being tested in phase three trials [30]. Each of these tracers possesses unique characteristics with their individual pros and cons pertaining (costs of) radionuclide production, physical half-life, image quality, radiation exposure, compatibility with exercise acquisition protocols, and tracer kinetics for quantification (Table. 11.1). None of the perfusion tracers excels on all of these features. Choice of tracer is therefore multifactorial and frequently depends on practical and logistical considerations.

### 11.3.1 Perfusion Tracer Characteristics

$H_2{}^{15}O$ is characterized by fundamentally different properties as compared with $^{82}$Rb, $^{13}NH_3$, and $^{18}$F-flurpiridaz [28, 31, 32]. $^{82}$Rb is a potassium analog that is rapidly and actively taken up by myocardial cells via the Na/K ATP transporter [33], whereas $^{13}NH_3$ is incorporated into the glutamine pool by active transport and passive diffusion processes [34]. $^{18}$F-flurpiridaz is a pyridazinone derivative that avidly binds to mitochondrial complex-1 [35]. The latter tracers are transported across the cell membrane and effectively become metabolically trapped while cleared from the intravascular compartment, yielding excellent qualitative gradable imaging due to high tissue-to-background ratios. In contrast, $H_2{}^{15}O$ is a freely diffusible, metabolically inert tracer that promptly reaches equilibrium between blood and tissue and is not accumulated in the myocardium. As a consequence, radiotracer distribution images of $H_2{}^{15}O$ are of little diagnostic value. The lack of diagnostic images has long prohibited the use of $H_2{}^{15}O$ for diagnostic imaging of CAD and virtually all studies on qualitative imaging for CAD have been conducted with $^{82}$Rb or $^{13}NH_3$ [36]. In recent years, however, digital subtraction techniques and parametric imaging by automated software packages now generate qualitative gradable $H_2{}^{15}O$

**Table 11.1** Characteristics of cardiac perfusion tracers

| | $H_2{}^{15}O$ | $^{13}NH_3$ | $^{82}Rb$ | $^{18}$F-flurpiridaz |
|---|---|---|---|---|
| Half-life | 123 s | 9.97 min | 76 s | 110 min |
| Production | Cyclotron | Cyclotron | Generator | Cyclotron |
| Kinetics | Freely diffusible, metabolically inert | Metabolically trapped in the myocardium | Metabolically trapped in the myocardium | Metabolically trapped in the myocardium |
| Mean positron range in tissue | 1.1 mm | 0.4 mm | 2.8 mm | 0.2 mm |
| Scan duration<br>Gating/LV function | 6 min<br>– | 20 min<br>+ | 6 min<br>+ | 20 min<br>+ |
| Radiation dose (3D) according to protocol in references | ~0.4 mSv/370 MBq | ~1 mSv/550 MBq | ~0.7 mSv/555 MBq<br>(2D: ~2.3 mSv/1,850 MBq) | ~2.1 mSv/111 MBq (rest)<br>~4.6 mSv/244 MBq (stress) |
| Exercise protocol compatible | – | – | – | + |
| Quantification | Excellent | Good | Moderate | Very good |
| Image quality | Good (parametric images) | Very good | Good | Excellent |

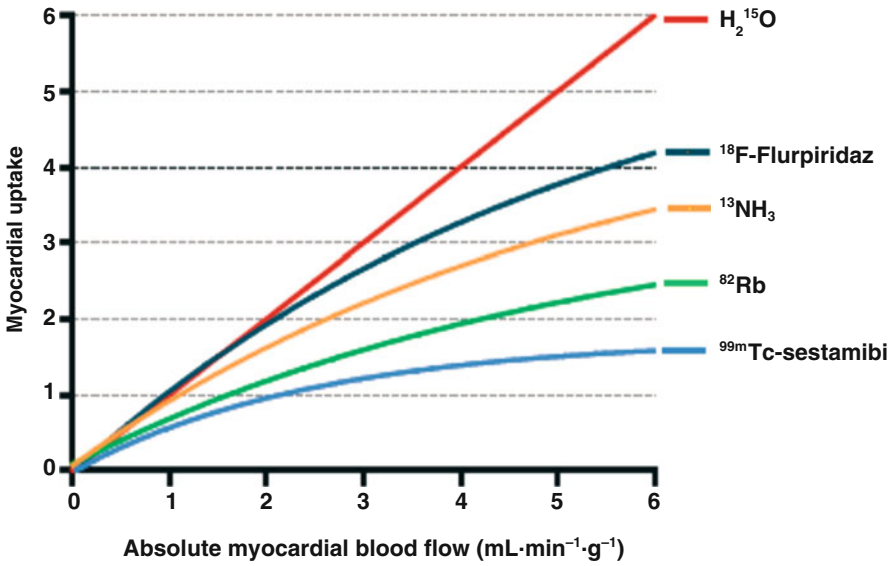


**Fig. 11.1** Kinetics of myocardial perfusion tracers; graphical presentation of the relationship between absolute myocardial blood flow of PET radiotracers and actual tracer uptake. 18F-flurpiridaz is not yet available for clinical use

perfusion images comparable to the aforementioned tracers [37–39]. These developments have enabled $H_2{}^{15}O$ to be utilized in clinical practice [40–42].

Next to relative uptake images, PET measures absolute levels of tracer concentration. Acquisition of PET in a dynamic fashion (i.e., multiple frames initiated upon administration of the tracer) generates time-activity curves of tracer flux between arterial blood and tissues [28]. This information allows to mathematically compute MBF in absolute terms (in units of $mL \cdot min^{-1} \cdot g^{-1}$) and calculate myocardial flow reserve (MFR). The ideal tracer accumulates in/or clears from the myocardium proportionally linear to perfusion, irrespective of flow rate or metabolic state [43]. $H_2{}^{15}O$ is the only tracer that meets these criteria and is therefore considered the gold standard for quantification of MBF [44]. An important limitation of the other aforementioned tracers is that myocardial extraction from arterial blood is incomplete and curvilinear with increasing flow rates, frequently referred to as the "roll-off" phenomenon (Fig. 11.1) [45].

This results in progressive underestimation of MBF measurements as actual flow increases. Correction models based on animal experiments can be employed yet induce noise, particularly when large correction factors are required with severely blunted extraction at high perfusion levels. Nonetheless, each of these tracers has been tested in animal experiments against microsphere-quantified perfusion, the invasive reference standard. $H_2{}^{15}O$ and $^{13}NH_3$ in particular have been well validated and display close agreement with microsphere flow and demonstrate low test-retest variability (10–15 %) [31, 44, 46–48]. Quantification of $^{82}Rb$ is less reliable as this

tracer harbors intrinsic limitations (ultrashort physical half-life, long positron range, and low extraction fraction). Nonetheless, recent studies have shown MBF measurements of $^{82}$Rb to be feasible [49]. Limited data are available pertaining the quantification of $^{18}$F-flurpiridaz, but its characteristics and kinetics should allow for highly reliable perfusion measurements [30, 43, 50].

### 11.3.2 Tracer Production and Availability

A pivotal issue that has proven to be the major obstacle for cardiac PET perfusion imaging is the necessity to produce the utilized tracers on-site. Of the currently available tracers, $H_2{}^{15}O$ and $^{13}NH_3$ require a cyclotron in the near proximity of the scanning facilities. $^{82}$Rb is produced by a $^{82}$Sr/$^{82}$Rb generator obviating the need for a cyclotron and is therefore more convenient to implement in clinical practice. The parent isotope $^{82}$Sr, however, needs to be replenished every 28 days at relatively high costs ($20.000). Therefore, high volume patient throughput is needed to be cost-effective. These issues of local tracer production have clearly limited the widespread use of cardiac perfusion PET. This may soon be overcome by the dawning perspective of fluorine-labeled tracers such as $^{18}$F-flurpiridaz [30]. Its longer physical half-life of 110 min allows for off-site production and could be as successful for cardiology as $^{18}$F-FDG PET has been for clinical oncology. Another advantage of $^{18}$F-labeled flow tracers is the fact that they allow to be used in physical exercise protocols whereby the radioisotope is administered during maximal exertion. $^{82}$Rb, $H_2{}^{15}O$, and $^{13}NH_3$ require injection while the patient is lying within the scanner, as tracer decay is too rapid to transport the patient from the treadmill or stationary bike to the scanner. These tracers can therefore only be utilized in conjunction with pharmacological stressor agents.

## 11.4 Diagnostic Accuracy and Prognosis

The vast majority of the studies on the diagnostic accuracy have been conducted with static uptake images of $^{82}$Rb and $^{13}NH_3$ [51]. Pooled analysis of these studies displays weighted sensitivity, specificity, NPV, and PPV which were 91, 86, 81, and 93 %, respectively, although it must be acknowledged that virtually all of these studies were compared with invasive coronary angiography without FFR and therefore lack an appropriate reference standard [14]. In comparison with single-photon emission computed tomography (SPECT) and cardiovascular magnetic resonance imaging (CMR), MPI with PET consistently yields the highest diagnostic accuracy [9–11]. Traditionally, these images (regardless of the utilized technique like SPECT, PET, CMR, or CT) are graded in a qualitative manner whereby perfusion defects are identified based on the relative distribution of the tracer. Unfortunately, conditions that are accompanied by lack of normal myocardium to act as reference limit such a qualitative approach and may yield false-negative results or underestimation of the extent of disease (e.g., in the case of multivessel disease and/or microvascular

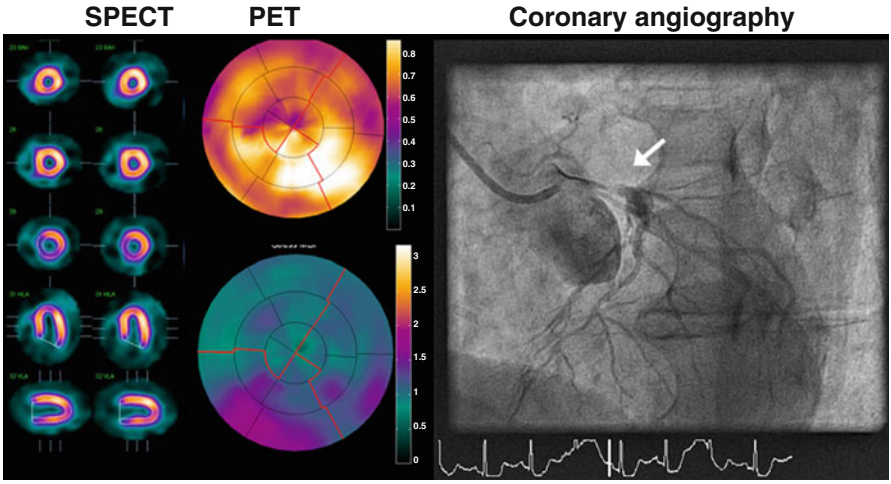


**Fig. 11.2** A 73-year-old male with atypical angina without cardiovascular risk factors, and no prior cardiac history was evaluated for coronary artery disease with 99mTc-sestamibi SPECT (*left panel rest* and *right panel stress*) and PET (*upper panel rest*, *lower panel stress*). Tracer distribution was homogenous during rest and stress on the SPECT images, and the visual and automated grading yielded a normal test result. Polar maps of PET displayed normal resting perfusion but diffusely blunted hyperemic MBF. Coronary angiography revealed a subtotal occlusion of the left main coronary artery (*white arrow*). SPECT imaging was false negative due to balanced ischemia, which was unmasked by the quantitative nature of the PET imaging

dysfunction). As already mentioned, PET offers the possibility to routinely quantify MBF and thus overcome these limitations (Fig. 11.2).

Indeed, there is mounting evidence that quantitative analysis with PET is superior to static uptake image grading [52–55]. Also compelling are the recent observations that hyperemic MBF quantification outperforms MFR to diagnose obstructive CAD, highlighting the potential of stress-only protocols [40, 42, 56, 57]. Reported thresholds of what should be considered pathological hyperemic MBF or MFR are unfortunately not uniform [51]. It appears that cutoff values are, at least in part, related to tracer kinetics and these should not be considered interchangeable [58]. Next to these technical issues, the detection of hemodynamically significant CAD is based on the presence of a flow-limiting epicardial coronary lesion, whereas PET measurements reflect the composite of perfusion throughout the entire coronary artery tree (roughly divided into the epicardial coronary compartment and the microvasculature) (see Fig. 11.3).

Definition of a single threshold will therefore remain elusive given its dependency on microvascular vasomotor function. The latter is related to age, gender, and cardiovascular risk profile [59, 60]. Nonetheless, recently, Danad et al. have explored optimal values for hyperemic MBF and MFR in a large multicenter trial using $H_2{}^{15}O$ PET whereby each patient was referred for invasive coronary angiography and FFR when appropriate [57]. Optimal thresholds were set at 2.3 $mL \cdot min^{-1} \cdot g^{-1}$ and 2.5 for hyperemic MBF and MFR, respectively. For hyperemic MBF, sensitivity,

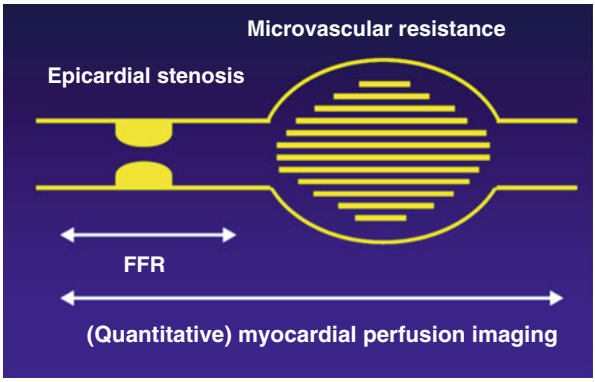


**Fig. 11.3** Graphical representation of the coronary vascular bed, divided into the epicardial conduit arteries and the microvasculature. The detection of coronary artery disease is based on the functional evaluation of an epicardial stenosis. Quantitative myocardial perfusion imaging provides an integrated measurement of perfusion of the entire coronary vascular bed, whereas, for example, fractional flow reserve (*FFR*) solely measures the pressure gradient across the coronary lesion. FFR and perfusion imaging therefore provide different information on coronary vascular health and are not necessarily concordant [51, 59]

specificity, and accuracy of hyperemic MBF for the detection of functionally relevant CAD were 87, 84, and 85 %, respectively. Of notice, these values were superior to MFR (84, 73, and 77 % for MFR, respectively) (Fig. 11.4). These data now pave the way for quantitative perfusion imaging, potentially with stress-only protocols, to be utilized in clinical practice.

In terms of prognosis, there is analogy to large-scale SPECT databases [61]. The extent and severity of (reversible) perfusion defects documented with PET hold strong prognostic information beyond traditional cardiovascular risk factors [51]. The quantitative nature of PET has shown incremental value. Of particular interest is the fact that apparent normal perfusion images with a homogenous tracer distribution can be reclassified based on diffusely blunted hyperemic MBF or MFR. Several studies have revealed that this subset of patients is at increased risk for future cardiac events [62–65].

## 11.5 Hybrid Cardiac PET/CT

Either an anatomical or functional approach in the evaluation of CAD has its limitations. Atherosclerosis is a gradual process that develops over decades. The advancing stages of CAD have been described by Glagov et al. [66]. Fig. 11.5 displays that noninvasive MPI with PET is particularly useful to document myocardial ischemia in advanced disease when coronary lesions become so tight that flow is hampered. In case of a normal scan, however, MPI PET cannot distinguish the different stages prior to the development of ischemia.

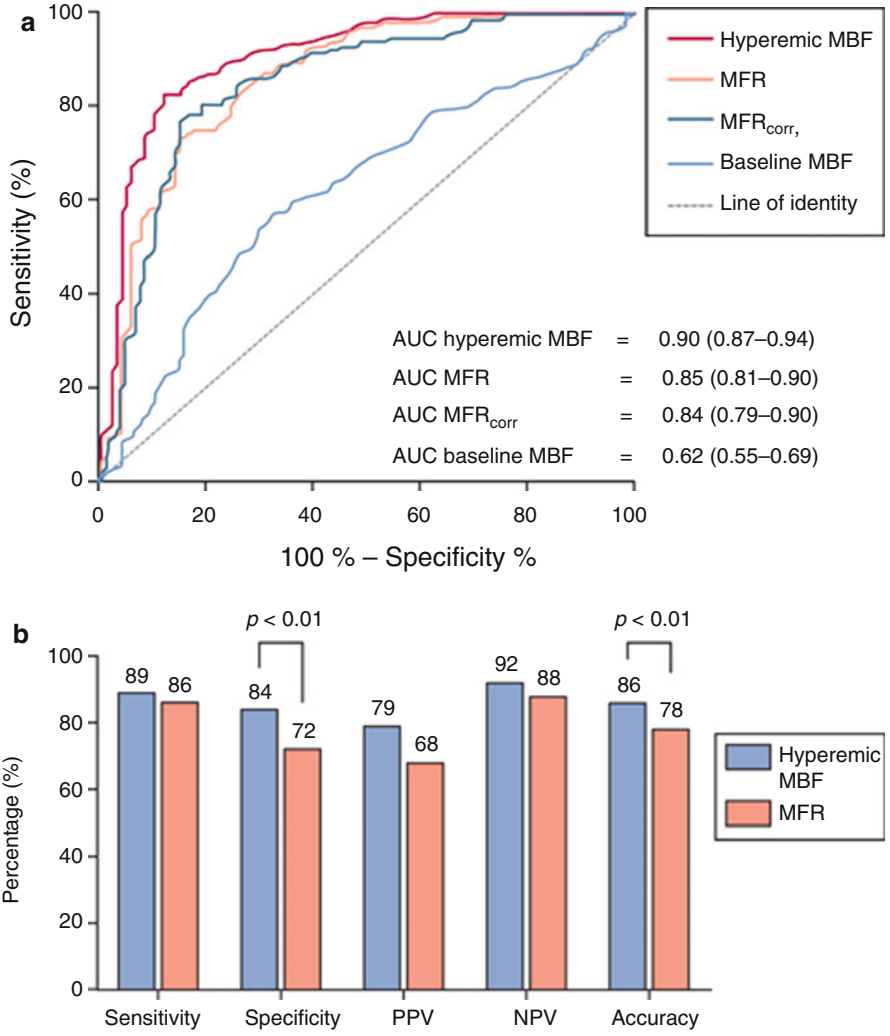


**Fig. 11.4** *Upper panel*: ROC curve analysis with corresponding AUCs and 95 % CI displaying the diagnostic performance of hyperemic MBF, MFR, MFRcorr, and baseline MBF for the detection of hemodynamically significant CAD as indicated by FFR per patient. *Lower panel*: sensitivity, specificity, PPV, NPV, and accuracy on a per-patient basis of quantitative PET MPI using hyperemic MBF and MFR, respectively, as a perfusion parameter (Adapted from Danad et al. [59])

Conversely, CCTA can accurately document the very early stages of coronary disease but does not have the ability to predict the hemodynamic consequences in more advanced stage of disease. Therefore, a hybrid assessment provides complementary rather than overlapping information. In recent years, CT technology has been fused with PET. These hybrid devices are now available up to 128-slice CT and state-of-the-art PET equipment, enabling the near simultaneous evaluation of

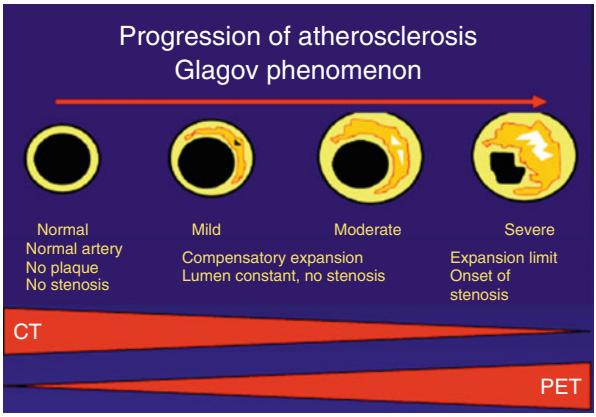


**Fig. 11.5** The gradual stages of coronary artery disease. CT-based angiography is particularly useful to document the early stages of disease, whereas PET perfusion only displays abnormalities in the later stages of disease. The combination of CT and PET therefore acts complimentary

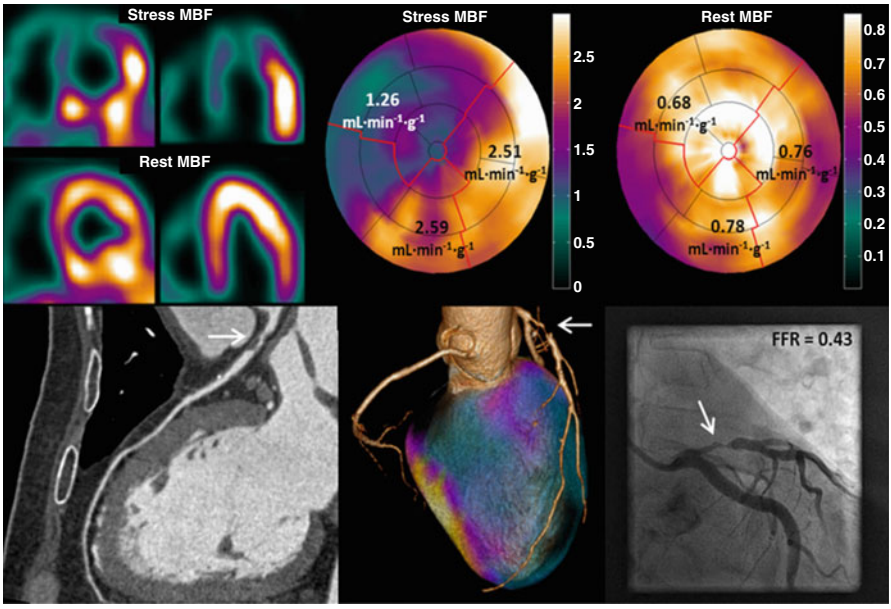


**Fig. 11.6** A 52-year-old male with atypical angina. Hybrid 15O-water PET/CTCA imaging reveals a severely reduced hyperemic perfusion (1.26 ml $\cdot$ min$^{-1}$ $\cdot$ g$^{-1}$) in the area supplied by the LAD artery with single-vessel disease documented with CCTA. Invasive coronary angiography can be planned with ad hoc percutaneous coronary intervention

coronary anatomy and quantitative myocardial perfusion in a single scanning session, which can be as short as 30 min (Fig. 11.6).

The number of studies on the diagnostic value of PET/CCTA for CAD is small yet convincingly demonstrates enhanced accuracy as compared with either modality alone (Table. 11.2) [40, 41, 67, 68]. Similar observations have been made in protocols of CCTA in conjunction with SPECT or CMR [69–73]. Hybrid imaging

**Table 11.2** Diagnostic performance of cardiac hybrid PET/CCTA imaging (results shown on a per-patient basis)

| Author | Hybrid PET/CT system | *N* | Reference standard for definition of obstructive CAD | Sensitivity CCTA/ PET/hybrid (%) | Specificity CCTA/ PET/hybrid (%) | NPV CCTA/PET/ hybrid (%) | PPV CCTA/PET/ hybrid (%) |
|---|---|---|---|---|---|---|---|
| Groves et al. [67] | $^{82}$Rb PET/64-slice CCTA | 33 | ICA > 50 % | 100/92/96 | 82/89/100 | 100/80/91 | 92/96/100 |
| Kajander et al. [41] | [$^{15}$O]$H_2O$ PET/64-slice CCTA | 107 | ICA > 50 % + FFR ≤ 0.80 | 95/95/95 | 87/91/100 | 97/97/98 | 81/86/100 |
| Danad et al. [40] | [$^{15}$O]$H_2O$ PET/64-slice CCTA | 120 | ICA > 50 % + FFR ≤ 0.80 | 100/76/76 | 34/82/92 | 100/83/84 | 51/76/86 |
| Thomassen et al. [68] | [$^{15}$O]$H_2O$ PET/64-slice CCTA | 44 | ICA > 50 % | 91/91/91 | 64/86/100 | 88/90/92 | 71/87/100 |
| Weighted summary | | 304 | | 97/89/90 | 67/87/98 | 96/88/91 | 74/86/97 |

*CCTA*, coronary computed tomography angiography, *CAD* coronary artery disease, *NPV* negative predictive value, *PPV* positive predictive value

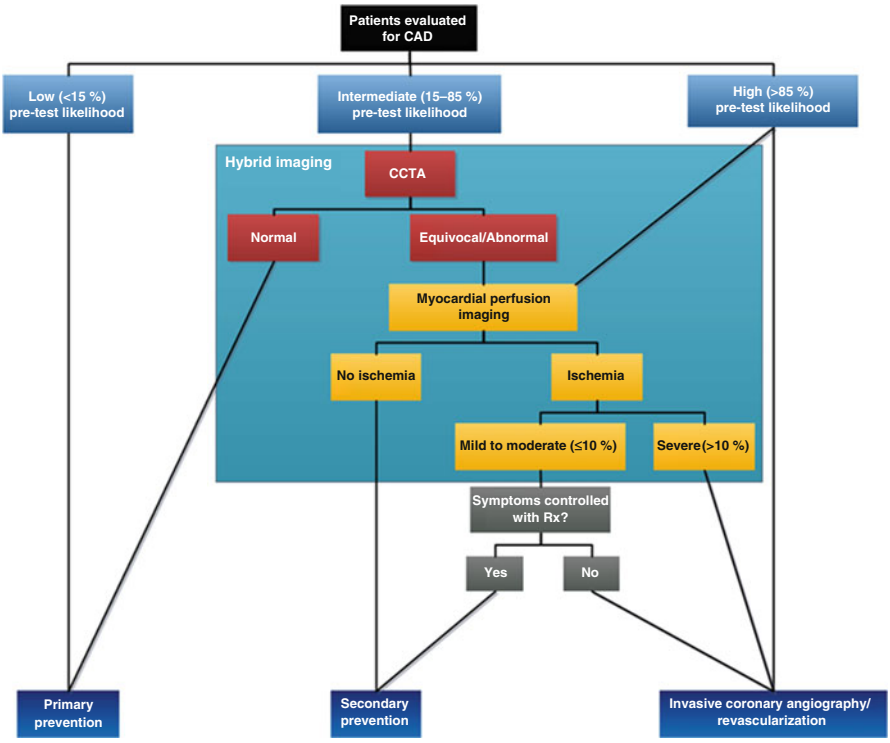


**Fig. 11.7** Proposed diagnostic algorithm for diagnosing CAD using CCTA and myocardial perfusion imaging

is shown to be particularly useful for enhancing the moderate specificity and PPV of CCTA.

Besides enhanced diagnostic value, profiling the anatomical and functional status of the coronary tree additionally yields incremental prognostic data. Combining coronary calcium scoring (CAC) with MPI adds prognostic value in patients with and without myocardial ischemia, although ischemia appears to be a more potent predictor of future cardiac events than coronary calcification [74, 75]. To date, studies on the prognostic relevance of PET combined with CCTA are lacking. Nevertheless, data obtained from hybrid SPECT/CCTA studies reveal a more accurate risk stratification of the combined anatomical and functional approach [76, 77]. The hybrid approach provides particular additional value to risk stratify patients when either functional or anatomical evaluation displays ambiguous results. In a large cohort of patients ($n=1{,}295$), Kim et al. recently highlighted that sequential imaging with SPECT and CCTA was of limited incremental prognostic value when either SPECT MPS or CCTA was clearly abnormal (i.e., SSS $\geq 4$ or CT-graded diameter stenosis $\geq 90$ %, respectively) [78]. Figure 11.7 displays a proposed algorithm for the diagnostic work-up for patients suspected of CAD. CCTA should be the initial test and be complemented with MPI in case of a documented coronary lesion or poor interpretable CT scan. MPI should subsequently act as gatekeeper for ICA. Adding routine quantitative MBF and MFR with PET appears to provide the most comprehensive diagnostic evaluation in this category of patients.

Even though steadily increasing, the availability of hybrid PET/CCTA is still limited. Therefore, latest efforts have been directed toward deriving physiological information from CT technology directly. Three methodological avenues are currently being explored. First, as adopted from well-defined CMR protocols, CT perfusion (CTP) by acquisition of a dynamic first pass (stress) sequence has demonstrated to be feasible. Although CTP is in its early development and still faces many technical issues, a recent multicenter trial utilizing 320-slice CT scanners demonstrated that CTP enhanced the diagnostic accuracy over CCTA alone [79]. Second, noninvasive estimation of FFR through computational fluid dynamics analysis solely based on the anatomical features of the coronary arteries obtained with CCTA has recently emerged [80]. Multicenter trials have shown that FFR-CT may indeed raise diagnostic accuracy of CCTA [81–83]. The model, however, is based on numerous assumptions and the overall incremental value appears to be limited [82]. Moreover, the tremendous computational complexity requires hours of off-line analysis hampering its implementation in clinical practice for the time being. Hence, a much simpler approach of this principle was proposed as a third option whereby contrast opacification along the course of a coronary artery is documented by linear regression. The rationale behind this so-called transluminal attenuation gradient (TAG) is that contrast opacification may in theory fall off more rapidly in the presence of a functionally significant stenosis than in the absence of stenosis [84]. Although elegant in its simplicity, the fundamental concept of these approaches whereby hyperemic functional consequences of a coronary lesion are attempted to be disclosed at baseline conditions is questionable and lacks additional diagnostic value over CCTA alone [85]. Clearly, deriving functional data from cardiac CT is work in progress.

## 11.6 Summary

Hybrid cardiac PET/CCTA allows for a comprehensive evaluation of patients suspected of coronary artery disease. Within a single session, complementary diagnostic information on anatomy and physiology is obtained to guide patient management in an optimal fashion. The added diagnostic and prognostic value of routine quantification of MBF and MFR is a feature that is unique for this type of advanced imaging. Although current evidence supports its use in clinical practice for appropriately selected patients, studies in larger cohorts and in multicenter setting are needed to further clarify unresolved issues like incremental value over alternative (hybrid) approaches, cost-effectiveness, and impact on patient outcome.

## References

1. Bashore TM, Bates ER, Berger PB, et al. American College of Cardiology/Society for Cardiac Angiography and Interventions Clinical Expert Consensus Document on cardiac catheterization laboratory standards. A report of the American College of Cardiology Task Force on Clinical Expert Consensus Documents. J Am Coll Cardiol. 2001;37(8):2170–214.
2. Pijls NH, De Bruyne B, Peels K, et al. Measurement of fractional flow reserve to assess the functional severity of coronary-artery stenoses. N Engl J Med. 1996;334:1703–8.

3. Tonino PAL, De Bruyne B, Pijls NHJ, et al. Fractional flow reserve versus angiography for guiding percutaneous coronary intervention. N Engl J Med. 2009;360:213–24.
4. De Bruyne B, Pijls NHJ, Kalesan B, et al. Fractional flow reserve-guided PCI versus medical therapy in stable coronary disease. N Engl J Med. 2012;367:991–1001.
5. Task Force Members, Montalescot G, Sechtem U, Achenbach S, et al. 2013 ESC guidelines on the management of stable coronary artery disease: the Task Force on the management of stable coronary artery disease of the European Society of Cardiology. Eur Heart J. 2013;34:2949–3003.
6. Schroeder S, Achenbach S, Bengel F, et al. Cardiac computed tomography: indications, applications, limitations, and training requirements: report of a Writing Group deployed by the Working Group Nuclear Cardiology and Cardiac CT of the European Society of Cardiology and the European Council of Nuclear Cardiology. Eur Heart J. 2008;29:531–56.
7. Shaw LJ, Marwick TH, Zoghbi WA, et al. Why all the focus on cardiac imaging? JACC Cardiovasc Imaging. 2010;3:789–94.
8. Danad I, Raijmakers PG, Harms HJ, et al. Effect of cardiac hybrid 15O-water PET/CT imaging on downstream referral for invasive coronary angiography and revascularization rate. Eur Heart J Cardiovasc Imaging. 2014;15:170–9.
9. Jaarsma C, Leiner T, Bekkers SC, et al. Diagnostic performance of noninvasive myocardial perfusion imaging using single-photon emission computed tomography, cardiac magnetic resonance, and positron emission tomography imaging for the detection of obstructive coronary artery disease: a meta-analysis. J Am Coll Cardiol. 2012;59:1719–28.
10. Parker MW, Iskandar A, Limone B, et al. Diagnostic accuracy of cardiac positron emission tomography versus single photon emission computed tomography for coronary artery disease: a bivariate meta-analysis. Circ Cardiovasc Imaging. 2012;5:700–7.
11. Mc Ardle BA, Dowsley TF, DeKemp RA, Wells GA, Beanlands RS. Does rubidium-82 PET have superior accuracy to SPECT perfusion imaging for the diagnosis of obstructive coronary disease? A systematic review and meta-analysis. J Am Coll Cardiol. 2012;60:1828–37.
12. Knaapen P, de Haan S, Hoekstra OS, et al. Cardiac PET-CT: advanced hybrid imaging for the detection of coronary artery disease. Neth Heart J. 2010;18:90–8.
13. Bogaard K, van der Zant FM, Knol RJJ, et al. High-pitch prospective ECG-triggered helical coronary computed tomography angiography in clinical practice: image quality and radiation dose. Int J Cardiovasc Imaging. 2014;31:1–9.
14. Danad I, Raijmakers PG, Knaapen P. Diagnosing coronary artery disease with hybrid PET/CT: it takes two to tango. J Nucl Cardiol. 2013;20:874–90.
15. Leber AW, Knez A, von Ziegler F, et al. Quantification of obstructive and nonobstructive coronary lesions by 64-slice computed tomography: a comparative study with quantitative coronary angiography and intravascular ultrasound. J Am Coll Cardiol. 2005;46:147–54.
16. Tonino PAL, Fearon WF, De Bruyne B, et al. Angiographic versus functional severity of coronary artery stenoses in the FAME study fractional flow reserve versus angiography in multivessel evaluation. J Am Coll Cardiol. 2010;55:2816–21.
17. Gaemperli O, Schepis T, Valenta I, et al. Functionally relevant coronary artery disease: comparison of 64-section CT angiography with myocardial perfusion SPECT. Radiology. 2008; 248:414–23.
18. Schuijf JD, Wijns W, Jukema JW, et al. Relationship between noninvasive coronary angiography with multi-slice computed tomography and myocardial perfusion imaging. J Am Coll Cardiol. 2006;48:2508–14.
19. Shreibati JB, Baker LC, Hlatky MA. Association of coronary CT angiography or stress testing with subsequent utilization and spending among Medicare beneficiaries. JAMA. 2011;306:2128–36.
20. Hachamovitch R, Nutter B, Hlatky MA, et al. Patient management after noninvasive cardiac imaging results from SPARC (Study of myocardial perfusion and coronary anatomy imaging roles in coronary artery disease). J Am Coll Cardiol. 2012;59:462–74.
21. Nielsen LH, Ortner N, Nørgaard BL, Achenbach S, Leipsic J, Abdulla J. The diagnostic accuracy and outcomes after coronary computed tomography angiography vs. conventional functional testing in patients with stable angina pectoris: a systematic review and meta-analysis. Eur Heart J Cardiovasc Imaging. 2014;15:961–71.

22. Hulten EA, Carbonaro S, Petrillo SP, Mitchell JD, Villines TC. Prognostic value of cardiac computed tomography angiography: a systematic review and meta-analysis. J Am Coll Cardiol. 2011;57:1237–47.
23. Min JK, Dunning A, Lin FY, et al. Age- and sex-related differences in all-cause mortality risk based on coronary computed tomography angiography findings results from the International Multicenter CONFIRM (Coronary CT Angiography Evaluation for Clinical Outcomes: An International Multicenter Registry) of 23,854 patients without known coronary artery disease. J Am Coll Cardiol. 2011;58:849–60.
24. Hadamitzky M, Täubert S, Deseive S, et al. Prognostic value of coronary computed tomography angiography during 5 years of follow-up in patients with suspected coronary artery disease. Eur Heart J. 2013;34:3277–85.
25. Blankstein R, Ferencik M. The vulnerable plaque: can it be detected with Cardiac CT? Atherosclerosis. 2010;211:386–9.
26. Versteylen MO, Kietselaer BL, Dagnelie PC, et al. Additive value of semiautomated quantification of coronary artery disease using cardiac computed tomographic angiography to predict future acute coronary syndrome. J Am Coll Cardiol. 2013;61:2296–305.
27. Motoyama S, Sarai M, Harigaya H, et al. Computed tomographic angiography characteristics of atherosclerotic plaques subsequently resulting in acute coronary syndrome. J Am Coll Cardiol. 2009;54:49–57.
28. Knaapen P, Camici PG, Marques KM, et al. Coronary microvascular resistance: methods for its quantification in humans. Basic Res Cardiol. 2009;104:485–98.
29. Knaapen P, Lubberink M. Cardiac positron emission tomography: myocardial perfusion and metabolism in clinical practice. Clin Res Cardiol. 2008;97:791–6.
30. Rischpler C, Park M-J, Fung GSK, Javadi M, Tsui BMW, Higuchi T. Advances in PET myocardial perfusion imaging: F-18 labeled tracers. Ann Nucl Med. 2012;26:1–6.
31. Iida H, Kanno I, Takahashi A, et al. Measurement of absolute myocardial blood flow with H215O and dynamic positron-emission tomography. Strategy for quantification in relation to the partial-volume effect. Circulation. 1988;78:104–15.
32. Schindler TH, Schelbert HR, Quercioli A, Dilsizian V. Cardiac PET imaging for the detection and monitoring of coronary artery disease and microvascular health. JACC Cardiovasc Imaging. 2010;3:623–40.
33. Huang SC, Williams BA, Krivokapich J, Araujo L, Phelps ME, Schelbert HR. Rabbit myocardial 82Rb kinetics and a compartmental model for blood flow estimation. Am J Physiol. 1989;256:H1156–64.
34. Schelbert HR, Phelps ME, Huang SC, et al. N-13 ammonia as an indicator of myocardial blood flow. Circulation. 1981;63:1259–72.
35. Yalamanchili P, Wexler E, Hayes M, et al. Mechanism of uptake and retention of F-18 BMS-747158-02 in cardiomyocytes: a novel PET myocardial imaging agent. J Nucl Cardiol. 2007;14:782–8.
36. Di Carli MF, Hachamovitch R. New technology for noninvasive evaluation of coronary artery disease. Circulation. 2007;115:1464–80.
37. Nesterov SV, Han C, Mäki M, et al. Myocardial perfusion quantitation with 15O-labelled water PET: high reproducibility of the new cardiac analysis software (Carimas). Eur J Nucl Med Mol Imaging. 2009;36:1594–602.
38. Harms HJ, Knaapen P, de Haan S, Halbmeijer R, Lammertsma AA, Lubberink M. Automatic generation of absolute myocardial blood flow images using [15O]H2O and a clinical PET/CT scanner. Eur J Nucl Med Mol Imaging. 2011;38:930–9.
39. Harms HJ, Nesterov SV, Han C, et al. Comparison of clinical non-commercial tools for automated quantification of myocardial blood flow using oxygen-15-labelled water PET/CT. Eur Heart J Cardiovasc Imaging. 2013;15(4):431–41.
40. Danad I, Raijmakers PG, Appelman YE, et al. Hybrid imaging using quantitative H215O PET and CT-based coronary angiography for the detection of coronary artery disease. J Nucl Med. 2013;54:55–63.
41. Kajander S, Joutsiniemi E, Saraste M, et al. Cardiac positron emission tomography/computed tomography imaging accurately detects anatomically and functionally significant coronary artery disease. Circulation. 2010;122:603–13.

42. Danad I, Raijmakers PG, Harms HJ, et al. Impact of anatomical and functional severity of coronary atherosclerotic plaques on the transmural perfusion gradient: a [15O]H2O PET study. Eur Heart J. 2014;35:2094–105.
43. Maddahi J. Properties of an ideal PET perfusion tracer: new PET tracer cases and data. J Nucl Cardiol. 2012;19 Suppl 1:S30–7.
44. Bergmann SR, Fox KA, Rand AL, et al. Quantification of regional myocardial blood flow in vivo with H215O. Circulation. 1984;70:724–33.
45. Saraste A, Kajander S, Han C, Nesterov SV, Knuuti J. PET: is myocardial flow quantification a clinical reality? J Nucl Cardiol. 2012;19:1044–59.
46. Bol A, Melin JA, Vanoverschelde JL, et al. Direct comparison of [13N]ammonia and [15O] water estimates of perfusion with quantification of regional myocardial blood flow by microspheres. Circulation. 1993;87:512–25.
47. Kaufmann PA, Gnecchi-Ruscone T, Yap JT, Rimoldi O, Camici PG. Assessment of the reproducibility of baseline and hyperemic myocardial blood flow measurements with 15O-labeled water and PET. J Nucl Med. 1999;40:1848–56.
48. Hutchins GD, Schwaiger M, Rosenspire KC, Krivokapich J, Schelbert H, Kuhl DE. Noninvasive quantification of regional blood flow in the human heart using N-13 ammonia and dynamic positron emission tomographic imaging. J Am Coll Cardiol. 1990;15:1032–42.
49. Lautamäki R, George RT, Kitagawa K, et al. Rubidium-82 PET-CT for quantitative assessment of myocardial blood flow: validation in a canine model of coronary artery stenosis. Eur J Nucl Med Mol Imaging. 2009;36:576–86.
50. Nekolla SG, Reder S, Saraste A, et al. Evaluation of the novel myocardial perfusion positron-emission tomography tracer 18F-BMS-747158-02: comparison to 13N-ammonia and validation with microspheres in a pig model. Circulation. 2009;119:2333–42.
51. Gould KL, Johnson NP, Bateman TM, et al. Anatomic versus physiologic assessment of coronary artery disease. Role of coronary flow reserve, fractional flow reserve, and positron emission tomography imaging in revascularization decision-making. J Am Coll Cardiol. 2013;62:1639–53.
52. Muzik O, Duvernoy C, Beanlands RS, et al. Assessment of diagnostic performance of quantitative flow measurements in normal subjects and patients with angiographically documented coronary artery disease by means of nitrogen-13 ammonia and positron emission tomography. J Am Coll Cardiol. 1998;31:534–40.
53. Kajander SA, Joutsiniemi E, Saraste M, et al. Clinical value of absolute quantification of myocardial perfusion with (15)O-water in coronary artery disease. Circ Cardiovasc Imaging. 2011;4:678–84.
54. Hajjiri MM, Leavitt MB, Zheng H, Spooner AE, Fischman AJ, Gewirtz H. Comparison of positron emission tomography measurement of adenosine-stimulated absolute myocardial blood flow versus relative myocardial tracer content for physiological assessment of coronary artery stenosis severity and location. JACC Cardiovasc Imaging. 2009;2:751–8.
55. Fiechter M, Ghadri JR, Gebhard C, et al. Diagnostic value of 13N-ammonia myocardial perfusion PET: added value of myocardial flow reserve. J Nucl Med. 2012;53:1230–4.
56. Joutsiniemi E, Saraste A, Pietilä M, et al. Absolute flow or myocardial flow reserve for the detection of significant coronary artery disease? Eur Heart J Cardiovasc Imaging. 2014;15:659–65.
57. Danad I, Uusitalo V, Kero T, et al. Quantitative assessment of myocardial perfusion in the detection of significant coronary artery disease: cutoff values and diagnostic accuracy of quantitative [(15)O]H2O PET imaging. J Am Coll Cardiol. 2014;64:1464–75.
58. Knaapen P. Quantitative myocardial blood flow imaging: not all flow is equal. Eur J Nucl Med Mol Imaging. 2014;41:116–8.
59. Danad I, Raijmakers PG, Appelman YE, et al. Coronary risk factors and myocardial blood flow in patients evaluated for coronary artery disease: a quantitative [15O]H2O PET/CT study. Eur J Nucl Med Mol Imaging. 2012;39:102–12.
60. Liga R, Rovai D, Sampietro T, et al. Insulin resistance is a major determinant of myocardial blood flow impairment in anginal patients. Eur J Nucl Med Mol Imaging. 2013;40:1905–13.

61. Shaw LJ, Iskandrian AE. Prognostic value of gated myocardial perfusion SPECT. J Nucl Cardiol. 2004;11:171–85.
62. Ziadi MC, DeKemp RA, Williams KA, et al. Impaired myocardial flow reserve on rubidium-82 positron emission tomography imaging predicts adverse outcomes in patients assessed for myocardial ischemia. J Am Coll Cardiol. 2011;58:740–8.
63. Herzog BA, Husmann L, Valenta I, et al. Long-term prognostic value of 13N-ammonia myocardial perfusion positron emission tomography added value of coronary flow reserve. J Am Coll Cardiol. 2009;54:150–6.
64. Farhad H, Dunet V, Bachelard K, et al. Added prognostic value of myocardial blood flow quantitation in rubidium-82 positron emission tomography imaging. Eur Heart J Cardiovasc Imaging. 2013;14:1203–10.
65. Fukushima K, Javadi MS, Higuchi T, et al. Prediction of short-term cardiovascular events using quantification of global myocardial flow reserve in patients referred for clinical 82Rb PET perfusion imaging. J Nucl Med. 2011;52:726–32.
66. Glagov S, Weisenberg E, Zarins CK, Stankunavicius R, Kolettis GJ. Compensatory enlargement of human atherosclerotic coronary arteries. N Engl J Med. 1987;316:1371–5.
67. Groves AM, Speechly-Dick M-E, Kayani I, et al. First experience of combined cardiac PET/64-detector CT angiography with invasive angiographic validation. Eur J Nucl Med Mol Imaging. 2009;36:2027–33.
68. Thomassen A, Petersen H, Diederichsen ACP, Mickley H, Jensen LO, Johansen A, et al. Hybrid CT angiography and quantitative 15O-water PET for assessment of coronary artery disease: comparison with quantitative coronary angiography. Eur J Nucl Med Mol Imaging. 2013;40:1894–904.
69. Rispler S, Keidar Z, Ghersin E, et al. Integrated single-photon emission computed tomography and computed tomography coronary angiography for the assessment of hemodynamically significant coronary artery lesions. J Am Coll Cardiol. 2007;49:1059–67.
70. Sato A, Nozato T, Hikita H, et al. Incremental value of combining 64-slice computed tomography angiography with stress nuclear myocardial perfusion imaging to improve noninvasive detection of coronary artery disease. J Nucl Cardiol. 2010;17:19–26.
71. Schaap J, Kauling RM, Boekholdt SM, et al. Incremental diagnostic accuracy of hybrid SPECT/CT coronary angiography in a population with an intermediate to high pre-test likelihood of coronary artery disease. Eur Heart J Cardiovasc Imaging. 2013;14:642–9.
72. Schaap J, de Groot JAH, Nieman K, et al. Added value of hybrid myocardial perfusion SPECT and CT coronary angiography in the diagnosis of coronary artery disease. Eur Heart J Cardiovasc Imaging. 2014;15(11):1281–8.
73. Groothuis JGJ, Beek AM, Brinckman SL, et al. Combined non-invasive functional and anatomical diagnostic work-up in clinical practice: the magnetic resonance and computed tomography in suspected coronary artery disease (MARCC) study. Eur Heart J. 2013;34:1990–8.
74. Schenker MP, Dorbala S, et al. Interrelation of coronary calcification, myocardial ischemia, and outcomes in patients with intermediate likelihood of coronary artery disease: a combined positron emission tomography/computed tomography study. Circulation. 2008;117:1693–700.
75. Naya M, Murthy VL, Foster CR, et al. Prognostic interplay of coronary artery calcification and underlying vascular dysfunction in patients with suspected coronary artery disease. J Am Coll Cardiol. 2013;61:2098–106.
76. van Werkhoven JM, Schuijf JD, Gaemperli O, et al. Prognostic value of multislice computed tomography and gated single-photon emission computed tomography in patients with suspected coronary artery disease. J Am Coll Cardiol. 2009;53:623–32.
77. Pazhenkottil AP, Nkoulou RN, Ghadri J-R, et al. Prognostic value of cardiac hybrid imaging integrating single-photon emission computed tomography with coronary computed tomography angiography. Eur Heart J. 2011;32:1465–71.
78. Kim H-L, Kim Y-J, Lee S-P, et al. Incremental prognostic value of sequential imaging of single-photon emission computed tomography and coronary computed tomography angiography in patients with suspected coronary artery disease. Eur Heart J Cardiovasc Imaging. 2014;15:878–85.

79. Rochitte CE, George RT, Chen MY, et al. Computed tomography angiography and perfusion to assess coronary artery stenosis causing perfusion defects by single photon emission computed tomography: the CORE320 study. Eur Heart J. 2014;35:1120–30.
80. Taylor CA, Fonte TA, Min JK. Computational fluid dynamics applied to cardiac computed tomography for noninvasive quantification of fractional flow reserve: scientific basis. J Am Coll Cardiol. 2013;61:2233–41.
81. Koo B-K, Erglis A, Doh J-H, et al. Diagnosis of ischemia-causing coronary stenoses by noninvasive fractional flow reserve computed from coronary computed tomographic angiograms. Results from the prospective multicenter DISCOVER-FLOW (Diagnosis of Ischemia-Causing Stenoses Obtained Via Noninvasive Fractional Flow Reserve) study. J Am Coll Cardiol. 2011;58:1989–97.
82. Min JK, Leipsic J, Pencina MJ, et al. Diagnostic accuracy of fractional flow reserve from anatomic CT angiography. JAMA. 2012;308:1237–45.
83. Nørgaard BL, Leipsic J, Gaur S, et al. Diagnostic performance of noninvasive fractional flow reserve derived from coronary computed tomography angiography in suspected coronary artery disease: the NXT trial (Analysis of Coronary Blood Flow Using CT Angiography: Next Steps). J Am Coll Cardiol. 2014;63:1145–55.
84. Wong DTL, Ko BS, Cameron JD, et al. Transluminal attenuation gradient in coronary computed tomography angiography is a novel noninvasive approach to the identification of functionally significant coronary artery stenosis: a comparison with fractional flow reserve. J Am Coll Cardiol. 2013;61:1271–9.
85. Stuijfzand WJ, Danad I, Raijmakers PG, et al. Additional value of transluminal attenuation gradient in CT angiography to predict hemodynamic significance of coronary artery stenosis. JACC Cardiovasc Imaging. 2014;7:374–86.